# S1 Patch aging scheme

The upscaling scheme used in FANv2 is based on a generic approach for evaluating the aggregate N fluxes for a distribution of patches based on the fluxes of a single patch. The main underlying assumptions are that

- Each patch has a well-defined age $a > 0$ which is equal to the time elapsed since the patch was created.
- The state of each patch is uniquely determined by its age $a$ and the current time $t$.
- The patches are aggregated over an area large enough that the distribution of the state variables can be approximated by integrable functions of $a$ and $t$.

Under these assumptions, the upscaling approach aims to link the evolution of the nitrogen content $N(t)$ of a single patch, given by a differential equation in the form

$$\frac{dN}{dt} = f(N, t), \tag{S1}$$

to an age and time dependent function $n(a, t)$ which describes how the nitrogen is distributed between the patches of different age.

We start by defining the density function $w(a, t)$ such that the surface area occupied by patches aged between $a$ and $a + \Delta a$ is given by

$$W(t) = \int_a^{a+\Delta a} w(a', t)da'. \tag{S2}$$

Since the quantities simulated by FANv2 are expressed as area densities, $W(t)$ is a fraction (area of patches / total area) and $w(a, t)$ has the unit $\mathrm{s}^{-1}$.

Any feature of the patches is now expressed as two-dimensional functions $\phi(a, t)$, and for every fixed age $a_0$, the single-variable functions

$$\Phi(t) = \phi(a_0 + t, t) \tag{S3}$$

define the evolution (Eq. S1) of an individual patch aged $a_0$ at $t = 0$. The total derivative of $\phi(a, t)$ can therefore be identified with the tendency of $\Phi$,

$$\frac{\partial \phi}{\partial a} + \frac{\partial \phi}{\partial t} = \frac{d\Phi}{dt}, \tag{S4}$$

where we substituted $\partial a/\partial t = 1$. Since FANv2 assumes that the area of a patch does not change with $a$, application of (S4) to the density function $w(a, t)$ yields a "continuity equation" for $w$:

$$\frac{\partial w}{\partial a} + \frac{\partial w}{\partial t} = 0. \tag{S5}$$

The equation (S1) governing the nitrogen density of a single patch can then be understood in the sense of Eq. (S4):

$$\frac{\partial N}{\partial t} + \frac{\partial N}{\partial a} = f(N, a, t). \tag{S6}$$

Combining Eqs. (S5) and (S6) yields and equation for the area-weighted N density $n(a, t) = w(a, t)N(a, t)$:

$$\frac{d}{dt}(wN) = \frac{\partial n}{\partial a} + \frac{\partial n}{\partial t} = w(a, t)f(N(a, t), a, t). \tag{S7}$$

If $f$ is linear with respect to $N$, Eq. (S7) simplifies to

$$\frac{\partial n}{\partial a} + \frac{\partial n}{\partial t} = f(n(a, t), a, t). \tag{S8}$$

Eq. (S7) is a hyperbolic first-order partial differential equation. Applying a first-order, forward-in-time discretization yields a two-step numerical scheme implemented in FANv2:

1. For each $i$, update $n_i(t)$ according to Eq. (S1) as

$$n_i(t') = n_i(t) + w_i(t)\overline{f\left(N_i(t), t\right)}\Delta t \tag{S9}$$

where $\Delta t$ denotes the time step and the tendency $\overline{f(N_i(t), t)}$ is evaluated as a mean over the $i$th age class.

2. Transfer nitrogen from the younger to older age classes according to

$$n_i(t + \Delta t) = \begin{cases} n_i(t') - \Delta t \frac{n_i(t')}{\Delta a_i}, i = 1 \\ n_i(t') - \Delta t \left( \frac{n_i(t')}{\Delta a_i} - \frac{n_{i-1}(t')}{\Delta a_{i-1}} \right), i > 1 \end{cases} \tag{S10}$$

where the ages $a_{i-1}$ and $a_i$ define the $i$th age class and $\Delta a_i = a_i - a_{i-1}$.

In FANv2, the tendency $f$ in Eq. (S1) is linear with respect to $N$. Substituting $N_i = n_i/w_i$ simplifies Eq. (S9) to

$$n_i(t') = n_i(t) + \overline{f\left(n_i(t), t\right)}\Delta t, \tag{S11}$$

and the area fractions $w_i$ are therefore not needed.

The fertilizer or manure N is initially introduced to the youngest age class, and subsequently transferred through the sequence of age classes as described by Eq. (S10), until reaching the final class $i*$. By Eq. (S10), nitrogen is removed from the final age class at a rate equal to $1/\Delta a_{i*}$, which can be made arbitrarily small by the choice of $\Delta a_{i*}$. In FANv2, the final bins have $\Delta a_{i*} = 360$ days, which sets the maximum age of the N patches considered. Although not implemented in the current version, the nitrogen aged beyond $\Delta a_{i*}$ could be transferred into the soil N pools in the CLM.

If the tendency $f(N, a, t)$ is nonlinear for $N$, Eq. (S7) requires evaluating the density function $w(a, t)$. This can be obtained from the exact solution to Eq. (S5),

$$w(a, t) = w(0, t - a), \tag{S12}$$

which is the area fraction occupied by fresh patches at time $t - a$. Alternatively, $w(a, t)$ could be evaluated numerically with a similar procedure as for $n(a, t)$, which has the advantage of guaranteeing consistency between the evolution of $w(a, t)$ and $n(a, t)$.

## S1.1 Application to moisture content

The framework described above can be used to aggregate the water budget for a class of patches. This is based on the assumption that the volumetric soil moisture of the patches can be expressed as a sum of a $t$-dependent background and an $a$-dependent perturbation:

$$\theta(a, t) = \theta_b(t) + \delta\theta(a). \tag{S13}$$

Applying Eq. (S4) to the single-patch water budget yields

$$\frac{d\theta}{dt} = \frac{\partial\theta}{\partial t} + \frac{\partial\theta}{\partial a} = \frac{q_{top} - q_{bot}}{\Delta z}, \tag{S14}$$

where $q_{top}$ and $q_{bot}$ are the water fluxes at the top and bottom of the layer with thickness $\Delta z$. Substituting Eq. (S13) and integrating Eq. (S14) over the age range $(a_i, a_{i+1})$ yields the budget averaged over the age class:

$$\overline{\frac{q_{top} - q_{bot}}{\Delta z}} = \overline{\frac{d\theta_b}{dt}} - \frac{\delta\theta(a_{i+1}) + \delta\theta(a_i)}{a_{i+1} - a_i}, \tag{S15}$$

where the lines denote $a$-averages, such as

$$\overline{q_{top}} = \frac{\int_{a_i}^{a_{i+1}} q_{top}\, da}{a_{i+1} - a_i}. \tag{S16}$$

# S2 Sub-models for pastures, slurry and synthetic fertilizers

## S2.1 Grazed pastures

The manure N excreted on pastures is represented by three age classes for TAN – G1, G2 and G3 – and the two organic N pools, GA and GR (Fig. 3 in the main text). The latter correspond to the available and resistant organic N fractions (see Section 2.2 in the main text). The TAN pools G1 and G2 represent fresh urine patches with elevated pH and water content, and the pool G3 represents feces and old urine patches, which are simulated without changes to the ambient soil pH or moisture. The ammoniacal nitrogen is continuously transferred from the younger to older TAN age classes according to Eq. (S10)

The age class G1 represents the conditions during the first 24 hours after deposition of urine. The evolution of pH in urine patches is prescribed based on the measurements of Vallis et al. (1982), Sherlock and Goh (1984) and Laubach et al. (2012); for G1, a peak pH of 8.5 is used. In addition to the elevated pH, the urine patches initially have a higher moisture content than the surrounding soil, which affects the diffusive fluxes (Eq. 7 in the main paper). The water content is assumed to relax back to the background soil level during the 24 h age span of G1.

Urine is assumed to instantly infiltrate the soil, and the initial ($a = 0$) volumetric water content of urine patches ($\mathrm{m^3 m^{-3}}$) is evaluated as

$$\theta_0 = \min(\theta_s, d_0/\Delta z + \theta_b), \tag{S17}$$

where $\theta_s$ is the volumetric water content at saturation, $d_0$ (m) is the ratio of urine volume to the area of a patch, and $\theta_b$ is the volumetric water content of unaffected soil. The parameter $d_0$ is likely to depend on the type of livestock; the value of 6 mm is adopted following Móring et al. (2016). If the soil layer becomes saturated, the excess urine is assumed to percolate directly to the underlying soil, and the corresponding fraction of TAN is not added to the TAN pool within FANv2.

Depending on ambient conditions, the relaxation from $\theta_0$ to $\theta_b$ may consist of evaporation or vertical or lateral transport of moisture. The possible lateral spreading of urine patches is ignored in FANv2. The N leaching flux $Q_p$ is evaluated by diagnosing the flux of soil water $q_p$ at the layer bottom from the water budget of the layer,

$$\overline{q_{top}} - \overline{q_p} = \Delta z \left( \overline{\frac{\partial \theta_b}{\partial t}} + \frac{\Delta \theta}{\Delta a} \right), \tag{S18}$$

where $\overline{q_{top}}$ is the net water flux (infiltration − evaporation) at the surface, the overbars denote averages over the age range $\Delta a$, and $\Delta\theta = \theta(a_{i+1}) - \theta(a_i)$. The tendency $\partial\theta_b/\partial t$ is common to all patches and evaluated within the hydrological scheme of CLM. FANv2 assumes that the evaporation rate of the urine patch can be approximated by that of the surrounding soil, so that $q_{top}$ is also taken from CLM.

Eq. (S18), derived in Section S1.1, states that the flux $q_p$ can be obtained from the water budget of the unaffected soil by adding the term $\Delta\theta/\Delta a$, which expresses the rate at which the perturbed soil moisture relaxes towards $\theta_b$. Since the relaxation is assumed to occur entirely within the 24 h age span of G1, $\Delta\theta = \theta_b - \theta_0$ for G1. The soil moisture for evaluating the soil resistances for pool G1 is set to the average of $\theta_0$ and $\theta_b$, corresponding to the midpoint of the age span.

The age class G2 spans the subsequent 10 days following G1. In typical conditions, this time is sufficient for the $NH_3$ flux from the surface to decrease to close to its background level (Sherlock and Goh, 1984; Laubach et al., 2012). As noted by Sherlock and Goh (1985), the soil pH remains elevated during this stage, and accordingly, a pH 8.0 is used for G2. The soil water content in G2 is kept equal to $\theta_b$, and thus $\Delta\theta = 0$ for G2.

The final TAN age class G3 represents the nitrogen remaining in urine patches after 11 days, but more importantly, G3 receives the mineralized TAN from the organic N pools GA and GR, which differ in their decomposition rate (Section 2.2). The pH value for G3 is assumed equal to the unaffected soil and taken from the Harmonized World Soil Database (HWSD; FAO and IIASA, 2009). This value is normally lower than the values prescribed for G1 and G2, and thus, the volatilization rate for the mineralized TAN is much lower than for urine. Similar to G2, $\Delta\theta = 0$ for G3.

## S2.2 Slurry

To derive the resistance for the slurry-covered soil, we first consider the generic situation depicted in Fig. S1, where a fraction of the slurry remains on the surface while the infiltrated fraction forms a water-saturated layer immediately below the soil surface. Instead of assuming a fixed layer thickness $\Delta z$, the fluxes for S0 are evaluated for the partly infiltrated slurry layer, and the layer thickness depends on infiltration and evaporation of the slurry. We do not track the distribution of TAN between the fractions above and below the surface, but do consider the two-layer structure when evaluating the resistances, as described below.

Following the resistance scheme in Fig. S1, the diffusive transport between the slurry-containing layer and surface is governed by the resistances $R_{\mathrm{ss}\uparrow}$ and $R_{\mathrm{sl}}$, which represent the aqueous phase diffusion in the saturated soil and in the slurry remaining on the soil surface. The downwards transport into soil is governed by the resistance $R_{\mathrm{ss}\downarrow}$ (aqueous phase diffusion in saturated soil) and the parallel resistances $R_{\mathrm{aq}\downarrow}$ and $R_{\mathrm{gas}\downarrow}$, which represent aqueous and gaseous diffusion in the unsaturated soil layer immediately below the saturated layer.

Denote the depth of the layer remaining on surface by $d_{sl}$ (m), and the depth of the saturated soil by $d_{sat}$. We assume that the volume of solid matter in slurry can be neglected. The total water volume ($\mathrm{m}^3\ \mathrm{m}^{-2}$) within the two layers is therefore

$$W = d_{sl} + d_{sat}\theta_s. \tag{S19}$$

As in Section 2.2, the resistances have the form $R = L_D/D$, where $D$ is diffusivity and $L_D$ denotes the length of the diffusion path. Normally in FANv2 (Eq. 8), $L_D$ is defined as half of the geometric thickness of the layer, $\Delta z/2$. However, when the water content $\theta$ within the TAN-containing layer changes rapidly, the mean TAN concentration $N_{\mathrm{TAN}}/W$ is a better approximation to the concentration at a depth $d_{1/2}$ such that

$$\int_0^{d_{1/2}} \theta(z)dz = \frac{1}{2}W, \tag{S20}$$

where $z = 0$ corresponds the slurry surface. It is understood that $\theta = 1$ within the uninfiltrated slurry, and $d_{1/2}$ thus divides the water volume $W$ into equal fractions. Fig. S1 assumes that $d_{sl} \leq W/2$, since, as shown below, this will always be the case in FANv2.

Following the notation defined above, the resistances in the slurry and the saturated layer are given as follows:

$$\begin{aligned} R_{\mathrm{sl}} &= \min(W/2, d_{sl})/D_{\mathrm{NH4}} \\ R_{\mathrm{ss}\uparrow} &= \frac{\max(W/2 - d_{sl}, 0)}{\theta_s \xi(\theta_s) D_{\mathrm{NH4}}} \\ R_{\mathrm{ss}\downarrow} &= \frac{W}{2\theta_s \xi(\theta_s) D_{\mathrm{NH4}}}, \end{aligned} \tag{S21}$$

where the tortuosity factor $\xi$ is applied to the molecular diffusivity $D_{\mathrm{NH4}}$ within soil but not to the slurry on surface ($R_{\mathrm{sl}}$). The remaining resistances ($R_a$, $R_b$, $R_{\mathrm{gas}\downarrow}$, and $R_{\mathrm{aq}\downarrow}$), and subsequently the nitrogen fluxes, are evaluated as in Section 2.2.

The depths $d_{sl}$ and $d_{sat}$ need to be determined for evaluating the resistances. At $a = 0$, $d_{sl}$ equals the slurry depth $d_0$, and at $a = \Delta a$, $d_{sl} = 0$. We assume that at $a = \Delta a/2$, half of the initial volume has infiltrated into the soil, so that

$$d_{sat}(a = \Delta a/2) = \frac{d_0}{2\varepsilon}. \tag{S22}$$

The depth $d_{sl}$ is obtained by subtracting the evaporation loss over $\Delta a/2$ from the remaining half of $d_0$:

$$d_{sl}(a = \Delta a/2) = \max\left(\frac{d_0 - \Delta a q_e}{2}, 0\right), \tag{S23}$$

which justifies the implicit assumption $d_{sl} \leq W/2$ in Fig. S1 and the Eqs. (S21).

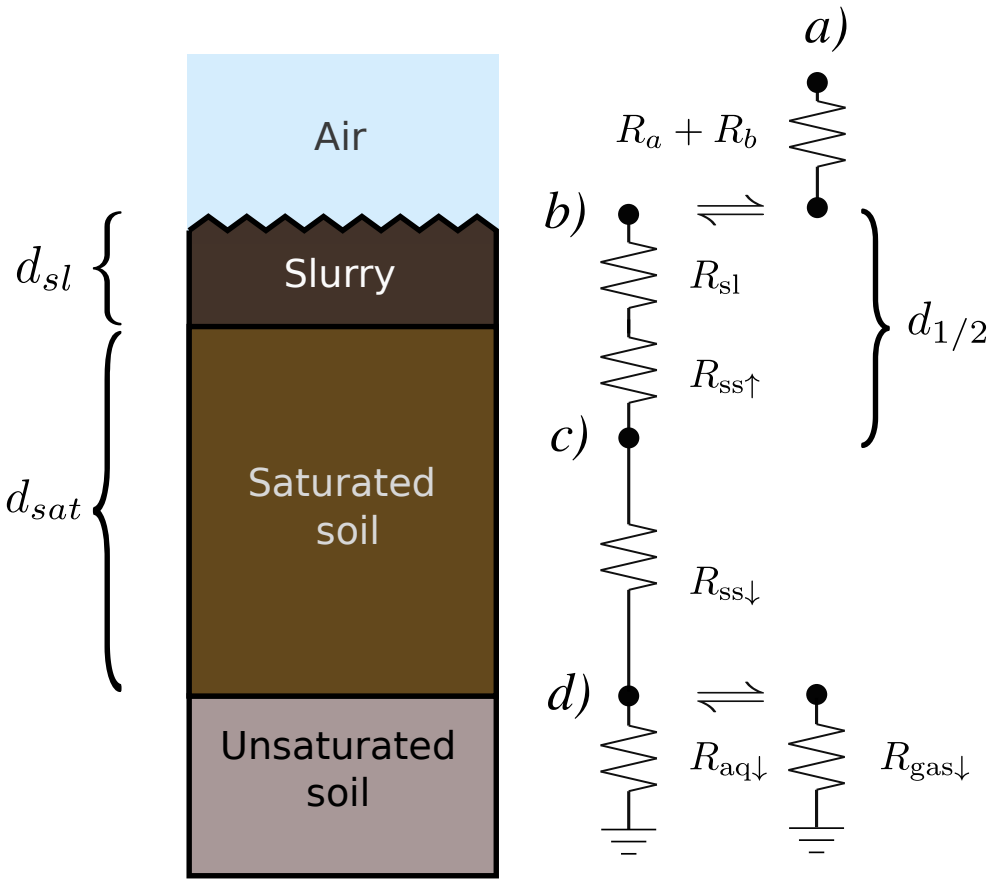


Figure S1: Schematic description and the corresponding resistance chart for modeling a partly infiltrated slurry layer. The resistance within the slurry remaining on surface is $R_{\mathrm{sl}}$, the resistances within saturated soil are denoted by $R_{\mathrm{ss}\uparrow}$ and $R_{\mathrm{ss}\downarrow}$; other resistances are as in Fig. 1. Labels a) to d) refer to TAN concentrations: a) [$NH_3$ (g)] at atmospheric reference height ; b) [$NH_3$ (g)] and [TAN(aq)] at the slurry surface; c) [TAN (aq)] in the slurry and saturated soil; d) [TAN (aq)] and [$NH_3$ (g)] at the bottom of the saturated soil layer. Thicknesses of the slurry and soil layers are denoted by $d_{sl}$, $d_{sat}$ and $d_{1/2}$ as described in the text.

The evaporation rate $q_e$ (m s$^{-1}$) for slurry is evaluated as

$$q_e = \frac{\rho_{air}}{\rho_w} \frac{Q_{sat} - Q_{atm}}{R_a + R_b}, \tag{S24}$$

where $\rho_{air}$ and $\rho_w$ are the densities of air and water, $Q_{atm}$ is specific humidity at the atmospheric reference height, $Q_{sat}$ is the specific humidity at saturation, and $R_a$ and $R_b$ are as in Eq. (6). The initial slurry depth $d_0$ is given by the slurry application rate (m$^3$ m$^{-2}$), and in the global simulations we assume $d_0 = 5$ mm, equal to 50 m$^3$ ha$^{-1}$.

The moisture flux $q_p$, required to evaluate the leaching flux (Eq. 9), is evaluated from the fraction of water in excess of $\Delta z \theta_s$ when the infiltration is complete,

$$q_p = \max\left(\frac{d_0 - \Delta a q_e - \Delta z \theta_s}{\Delta a}, 0\right). \tag{S25}$$

where the cumulative evaporation is subtracted from the initial water volume.

The pH of slurry tends to increase after application due to volatilization of $CO_2$; a constant value 8.0 is used for pools S1 and S2 based on the data published by Sommer and Olesen (1991), Bussink et al. (1994) and Sherlock et al. (2002). Similar to G3, the pH for S3 is taken from the HWSD database.

### S2.3 Synthetic fertilizers

Three TAN age classes (F1, F2 and F3) and two urea age classes (U1 and U2) are used to evaluate the volatilization losses for urea fertilizers (Fig. 3). The peak pH following urea application is often between 8 and 9 (Black et al., 1985; Whitehead and Raistrick, 1990; Sommer, 2013), and pHs of 7.0, 8.5 and 8.0 were chosen for F1, F2 and F3.

## S3 Nitrogen inputs

### S3.1 Manure N excretion

The estimated nitrogen excretion of livestock is based on the coefficients and animal weights in IPCC (2006). The yearly N excretion rates are listed in Table S1. For cattle, the coefficients are given for dairy and other cattle; the average is evaluated assuming 26 % fraction of dairy cattle for Europe, North America and Oceania , 35 % for India, and 14 % for other regions. The dairy cattle fraction for India is based on statistics published by the Indian Ministry of Agriculture and Farmers Welfare (2015), for other regions, the fraction is adapted from Bouwman et al. (1997). Geographical distributions of manure N in pastoral and landless production systems are shown in Fig. S2.

### S3.2 Fertilizers

As noted in the main text (Section 2.5.2), the N fertilizer application in the simulations is prescribed in the CLM input dataset (Lawrence et al., 2016). The disaggregation to urea, ammonium, and nitrate N was based on the consumption statistics of the International Fertilizer Association (IFA) for the year 2013. The country-level values were used to derive gridded maps of fraction of urea and nitrate N. For countries with missing data for urea, the fraction was extrapolated from the neighboring areas. To ensure that the sum of urea and nitrate fraction remains below 1, the nitrate fraction was not extrapolated but assumed zero when missing. Maps of urea and other fertilizer use are shown in Fig. S3.

## S4 Grazing and housing periods in mixed systems

Ruminants in mixed/landless systems are assumed to graze when the 10-day mean daily minimum temperature exceeds +10° C. At other times the livestock is assumed to remain in animal housings. Fig. S4 shows the number of yearly housing days estimated using the temperature threshold and

Table S1: Nitrogen excretion coefficients for livestock, kgN $yr^{-1}$ head $^{-1}$.

| | North America | Western Europe | Eastern Europe | Oceania | Latin America | Africa | Middle East | Asia | India |
|---|---|---|---|---|---|---|---|---|---|
| Cattle, average | 58.0 | 65.0 | 55.3 | 65.5 | 44.2 | 42.6 | 52.7 | 42.4 | 25.4 |
| Dairy cattle | 97.0 | 105.1 | 70.3 | 80.3 | 70.1 | 60.2 | 70.3 | 60.0 | 47.2 |
| Other cattle | 44.0 | 50.6 | 50.0 | 60.2 | 40.1 | 39.8 | 49.9 | 39.6 | 13.7 |
| Pigs, average | 11.2 | 16.1 | 17.0 | 15.6 | 16.8 | 16.8 | 16.8 | 5.1 | 5.1 |
| Market swine | 7.1 | 9.3 | 10.0 | 8.7 | 16.0 | 16.0 | 16.0 | 4.3 | 4.3 |
| Breeding swine | 17.3 | 30.4 | 30.2 | 30.2 | 5.6 | 5.6 | 5.6 | 2.5 | 2.5 |
| Poultry | 0.5 | 0.5 | 0.5 | 0.5 | 0.5 | 0.5 | 0.5 | 0.5 | 0.5 |
| Sheep | 7.4 | 15.0 | 15.9 | 20.0 | 12.0 | 12.0 | 12.0 | 12.0 | 12.0 |
| Goats | 6.3 | 18.0 | 18.0 | 20.0 | 15.0 | 15.0 | 15.0 | 15.0 | 15.0 |
| Buffalo | 44.4 | 44.4 | 44.4 | 44.4 | 44.4 | 44.4 | 44.4 | 44.4 | 34.5 |

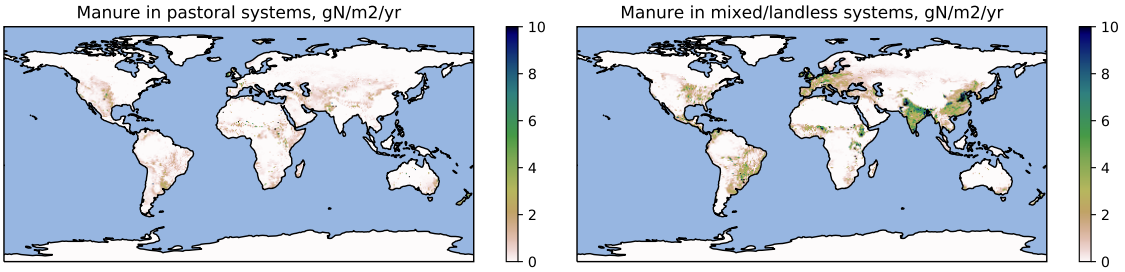


Figure S2: Manure N production (gN $m^{-2}yr^{-1}$) in pastoral (left) and mixed/landless systems (right).

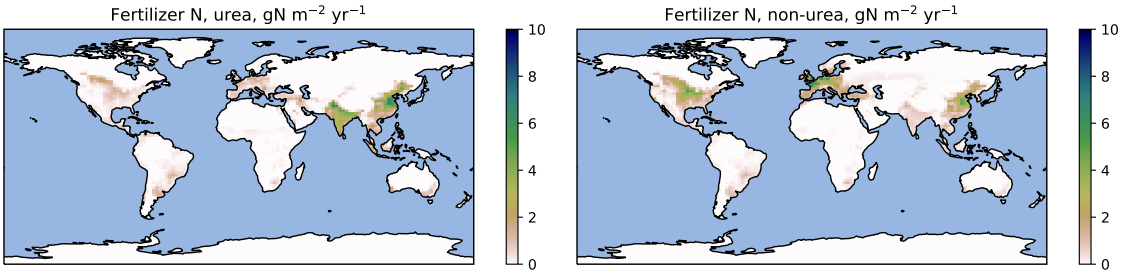


Figure S3: Yearly application (gN $m^{-2}yr^{-1}$) of urea (left) and other N fertilizers (right).

global temperature data from the NCEP reanalyses for 1980-2010. Fig. S5 compares the yearly housing days for Europe with the survey results (for cattle) reported by Klimont and Brink (2004). The values shown for European countries are weighted averages; the distribution of housing days was weighted by the population distribution of cattle within each country.

# S5 Sensitivity experiments

The sensitivity to model parameters was examined with experiments consisting of 2-year CLM simulations forced by the GSWP3 dataset. The experiments, the modified parameters, and changes in $NH_3$ emission are listed in Table S2. Switching the meteorological forcing from the CAM simulation to GSWP3 changed to total emission by $\sim$2 %; all other changes in emissions are reported with regard to the GSWP3-driven control simulation.

In the experiments evaluating sensitivity to the layer thickness $\Delta z$, only the thickness used in FAN computations was changed; the soil layers used in elsewhere in CLM were not changed. The water content used in FAN computations was taken for the topmost CLM layer in all experiments.

The sensitivity to manure TAN fraction by was evaluated by computing the emissions at 0 and 100 % TAN fractions. Since the model is linear with respect to N input, this allows calculating the $NH_3$ volatilization for any TAN fraction $f_{\mathrm{TAN}}$ as

$$F_M(f_{\mathrm{TAN}}) = f_{\mathrm{TAN}} \times F_M(f_{\mathrm{TAN}} = 1) + (1 - f_{\mathrm{TAN}}) \times F_M(f_{\mathrm{TAN}} = 0), \tag{S26}$$

where $F_M$ denotes the total $NH_3$ emission from manure. In the experiments, $F_M(0) = 6.8$ Tg N and $F_M(1) = 56$ Tg N. Varying the TAN fraction between 40 and 80 % would therefore result in about $\pm$10 TgN variation in the global $NH_3$ emission.

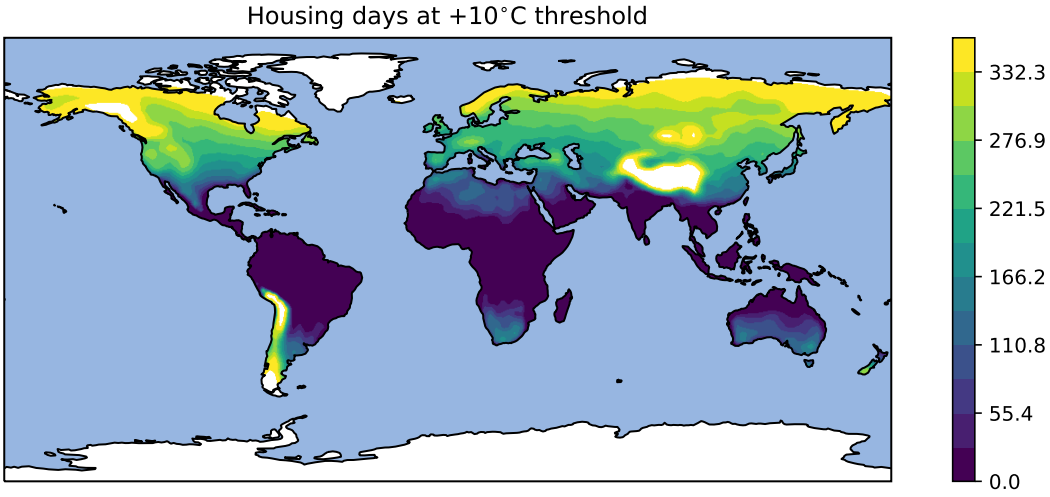


Figure S4: Average number of housing days per year estimated using the 1980-2010 NCEP temperature reanalyses.

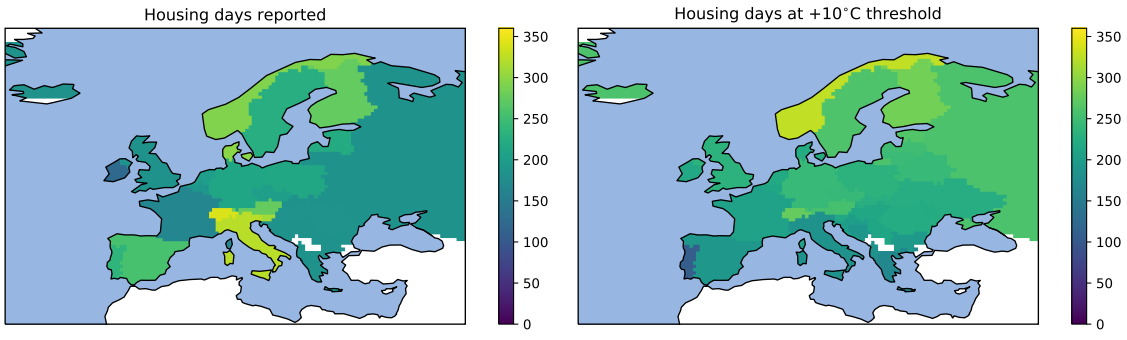


Figure S5: Yearly housing days reported by Klimont and Brink (2004) (left) and estimated using a temperature threshold (right).

Table S2: Relative changes in $NH_3$ emissions in the sensitivity experiments. The change for the control run is relative to the main run; for other experiments the change with respect to the control run is shown. Percent change in emission per percent change in parameter is shown in parentheses when applicable.

| | | Percent difference in $NH_3$ emission | | | | | | | | | | |
|---|---|---|---|---|---|---|---|---|---|---|---|---|
| Parameter | Value | Africa | Asia except China and India | China | Europe | India | Latin America | North America | Oceania | World | | |
| | | | | | | | | | | Total | Fertilizer | Manure |
| Control[1] | | +8 | +2 | −0 | −1 | +1 | +4 | +4 | +1 | +2 | +6 | +1 |
| $\tau_{\text{infl}}$[2] | ×0.5 | −2 | −2 | −3 | −5 | −2 | −3 | −3 | −3 | −3 (+0.1) | +0 | −3 (+0.1) |
| | ×2.0 | +2 | +3 | +5 | +6 | +2 | +3 | +4 | +4 | +3 (+0.0) | +0 | +4 (+0.0) |
| $d_0$ for urine [3] | −2 mm | +7 | +4 | +2 | +1 | +4 | +5 | +2 | +4 | +4 (−0.1) | +0 | +5 (−0.1) |
| | +2 mm | −6 | −3 | −2 | −1 | −3 | −5 | −2 | −5 | −3 (−0.1) | +0 | −4 (−0.1) |
| pH for manure[4] | +0.5 | +9 | +8 | +8 | +12 | +6 | +9 | +9 | +19 | +9 | +0 | +11 |
| | −0.5 | −8 | −6 | −6 | −10 | −4 | −7 | −7 | −11 | −7 | +0 | −9 |
| $f_{\text{TAN}}$[5] | 0 | −70 | −62 | −57 | −77 | −46 | −72 | −54 | −64 | −63 (+0.6) | +0 | −81 (+0.8) |
| | 1 | +46 | +42 | +38 | +52 | +31 | +48 | +36 | +43 | +42 (+0.6) | +0 | +54 (+0.8) |
| pH for other fert.[6] | 7 | +1 | +2 | +1 | +8 | +0 | +3 | +11 | +0 | +3 | +12 | +0 |
| pH for urea[7] | | −0 | −0 | +2 | −1 | +1 | −2 | −0 | +2 | +0 | +1 | +0 |
| Urea decomp.[8] | ×0.5 | +0 | +2 | +4 | +1 | +3 | +1 | +3 | +2 | +2 (−0.0) | +9 (−0.2) | +0 |
| | ×2.0 | −0 | −3 | −5 | −2 | −4 | −2 | −3 | −2 | −3 (−0.0) | −11 (−0.1) | +0 |
| Fert. timing[9] | 1 day | +0 | −2 | −0 | +2 | −4 | +0 | +1 | −1 | −1 | −3 | +0 |
| | 90 days | −1 | +4 | −6 | −2 | +0 | −1 | +2 | +5 | −0 | −2 | +0 |
| $\Delta z$[10] | ×0.5 | +5 | +12 | +22 | +19 | +13 | +13 | +29 | +24 | +15 (−0.3) | +41 (−0.8) | +7 (−0.1) |
| | ×2.0 | −28 | −26 | −27 | −20 | −30 | −24 | −31 | −33 | −27 (−0.3) | −52 (−0.5) | −19 (−0.2) |
| $K_d$[11] | 0 | +9 | +12 | +20 | +17 | +13 | +16 | +21 | +24 | +15 (−0.2) | +30 (−0.3) | +11 (−0.1) |
| | ×10.0 | −35 | −31 | −38 | −32 | −36 | −34 | −40 | −43 | −35 (−0.0) | −55 (−0.1) | −29 (−0.0) |
| Fraction of grazing[12] | +0.30 | −17 | −12 | −8 | −6 | −19 | −20 | −5 | −15 | −14 (−0.3) | +0 | −18 (−0.4) |
| | −0.30 | +17 | +12 | +8 | +7 | +19 | +21 | +5 | +15 | +14 (−0.3) | +0 | +18 (−0.4) |

[1]Control run with GSWP3 forcing. [2]Slurry infiltration time. [3]See Section S2.1. [4]Add or subtract from pH of N classes G1–G3 and S0–S3 . [5]Fraction of TAN in manure. [6]Fixed pH for age class F4. [7]pH for N classes F1, F2, F3 set to soil pH + 0.5, 2, 1.5 units. [8]Time constant $1/k_U$. [9]Fertilizer application window, days from leaf emergence. [10]Soil layer thickness. [11]Adsorption constant. [12]Maximum fraction of ruminants grazing in mixed production systems.

## S6 Sensitivity to mean temperature and precipitation

The sensitivity of $NH_3$ emissions to mean temperature was investigated with a linear regression on the geographical distribution of the simulated emissions. The model grid cells were first categorized by yearly rainfall, and then, the normalized volatilization loss ($NH_3$ emitted / N applied) within each category was fit with a linear function of the yearly mean temperature, assuming that for each grid cell,

$$NH_3/N_{appl} = a + bT + r \tag{S27}$$

where $a$ and $b$ are the regression parameters, $T$ is the temperature (°C) and the residual $r$ represents the temperature-independent effects. The temperature sensitivity is obtained from Eq. (S27) as

$$\Delta(NH_3) = bN_{appl}\Delta T. \tag{S28}$$

The temperature sensitivity of the total emission is then obtained by summing Eq. (S28) over the gridcells and precipitation categories.

The regression was evaluated separately for manure, urea, and other synthetic fertilizers. Exponential fits were tested in addition to the linear fits, however, the exponential fits invariably had lower $R^2$ than the linear fits and thus were not analyzed further. Results of the regression and the temperature response are shown in Table S3.

Table S3: Parameters of linear fits of the normalized volatilization loss (N emitted / N applied) as function of local mean temperature in °C. Present day manure N production or fertilizer N application and the corresponding $NH_3$ emissions are shown for each category.

| Source | Precipitation, mm | Intercept | Slope, $K^{-1}$ | $R^2$ | N applied, Tg | $NH_3$ emitted, Tg N | Temperature sensitivity, % $K^{-1}$ |
|---|---|---|---|---|---|---|---|
| Manure | < 200 | 0.13 | 0.009 | 0.87 | 8.5 | 2.9 | 2.5 |
| | 200 – 500 | 0.15 | 0.008 | 0.65 | 20.8 | 6.4 | 2.5 |
| | 500 – 1000 | 0.18 | 0.006 | 0.40 | 41.1 | 12.5 | 1.9 |
| | 1000 – 2000 | 0.19 | 0.005 | 0.18 | 36.4 | 11.2 | 1.7 |
| | > 2000 | 0.15 | 0.006 | 0.07 | 12.8 | 3.6 | 2.0 |
| | Total | | | | 119.6 | 36.5 | 2.0 |
| Urea | < 200 | 0.20 | 0.005 | 0.05 ($p = 0.01$) | 3.1 | 0.6 | 2.4 |
| | 200 – 500 | 0.00 | 0.013 | 0.48 | 8.5 | 1.6 | 7.1 |
| | 500 – 1000 | -0.03 | 0.014 | 0.70 | 13.1 | 2.4 | 7.5 |
| | 1000 – 2000 | 0.00 | 0.010 | 0.45 | 12.8 | 2.8 | 4.7 |
| | > 2000 | 0.04 | 0.005 | 0.09 | 4.7 | 0.7 | 3.2 |
| | Total | | | | 42.2 | 8.1 | 5.7 |
| Other fert. | < 200 | -0.01 | 0.010 | 0.29 | 1.0 | 0.2 | 6.1 |
| | 200 – 500 | -0.05 | 0.010 | 0.33 | 7.7 | 0.8 | 9.3 |
| | 500 – 1000 | -0.05 | 0.007 | 0.34 | 20.9 | 1.4 | 10.8 |
| | 1000 – 2000 | -0.04 | 0.005 | 0.22 | 8.2 | 0.5 | 9.0 |
| | > 2000 | 0.00 | 0.001 | 0.03 ($p = 0.02$) | 2.6 | 0.1 | 4.1 |
| | Total | | | | 40.4 | 2.9 | 9.7 |
| All sources | Total | | | | 202.1 | 47.5 | 3.1 |

# References


Black, A. S., Sherlock, R. R., Smith, N. P., Cameron, K. C., and Goh, K. M. (1985). Effects of form of nitrogen, season, and urea application rate on ammonia volatilisation from pastures. *New Zealand Journal of Agricultural Research*, 28(4):469–474.

Bouwman, A. F., Lee, D. S., Asman, W. A., Dentener, F. J., Van Der Hoek, K. W., and Olivier, J. G. (1997). A global high-resolution emission inventory for ammonia. *Global Biogeochemical Cycles*, 11(4):561–587.

Bussink, D. W., Huijsmans, J. F. M., and Ketelaars, J. J. M. H. (1994). Ammonia volatilization from nitric-acid-treated cattle slurry surface applied to grassland.

FAO/IIASA/ISCRIC/IIS-CAS/JRC (2009). Harmonized World Soil Database (version 1.1).

IMA (2015). Basic animal husbandry and fisheries statistics 2015. Technical report, Government of India, Ministry of Agriculture.

IPCC (2006). *2006 IPCC Guidelines for National Greenhouse Gas Inventories*. IGES, Japan.

Klimont, Z. and Brink, C. (2004). Modeling of emissions of air pollutants and greenhouse gases from agricultural sources in Europe. Technical report, International Institute for Applied Systems Analysis.

Laubach, J., Taghizadeh-Toosi, A., Sherlock, R. R., and Kelliher, F. M. (2012). Measuring and modelling ammonia emissions from a regular pattern of cattle urine patches. *Agricultural and Forest Meteorology*, 156:1–17.

Lawrence, D. M., Hurtt, G. C., Arneth, A., Brovkin, V., Calvin, K. V., Jones, A. D., Jones, C. D., Lawrence, P. J., de Noblet-Ducoudré, N., Pongratz, J., and Others (2016). The Land Use Model Intercomparison Project (LUMIP) contribution to CMIP6: rationale and experimental design. *Geoscientific Model Development*, 9(9):2973–2998.

Móring, A., Vieno, M., Doherty, R. M., Laubach, J., Taghizadeh-Toosi, A., and Sutton, M. A. (2016). A process-based model for ammonia emission from urine patches, GAG (Generation of Ammonia from Grazing): description, validation and sensitivity analysis. *Biogeosciences*, 13:1837–1861.

Sherlock, R. and Goh, K. (1984). Dynamics of ammonia volatilization from simulated urine patches and aqueous urea applied to pasture. I. Field Experiments. *Fertilizer Research*, 5:181–195.

Sherlock, R. R. and Goh, K. M. (1985). Dynamics of ammonia volatilization from simulated urine patches and aqueous urea applied to pasture. II. Theoretical derivation of a simplified model. *Fertilizer Research*, 6:3–22.

Sherlock, R. R., Sommer, S. G., Khan, R. Z., Wood, C. W., Guertal, E. A., Freney, J. R., Dawson, C. O., and Cameron, K. C. (2002). Ammonia, Methane and Nitrous Oxide Emission from Pig Slurry Applied to a Pasture in New Zealand. *J. Environ. Qual.*, 31:1491–1501.

Sommer, S. G. (2013). *Ammonia volatilisation from livestock slurries and mineral fertilisers*. PhD thesis, Syddansk Universitet.

Sommer, S. G. and Olesen, J. E. (1991). Effects of Dry Matter Content and Temperature on Ammonia Loss from Surface-Applied Cattle Slurry. *J. Environ. Qual.*, 20:679–683.

Vallis, L., Harper, A., Catchpoole, V. R., and Weier, K. L. (1982). Volatilization of ammonia from urine patchcs in a subtropical pasture. *Australian Journal of Agricultural Research*, 33(1):97–107.

Whitehead, D. C. and Raistrick, N. (1990). Ammonia volatilization from five nitrogen compounds used as fertilizers following surface application to soil. *J. Soil Sci.*, 41:387–394.